



Geophysical characterization of areas prone to quick-clay landslides using radio-magnetotelluric and seismic methods



Shunguo Wang ^a, Alireza Malehmir ^a, Mehrdad Bastani ^b

^a Department of Earth Sciences, Uppsala University, Villavägen 16, SE 75236, Uppsala, Sweden

^b Geological Survey of Sweden, Villavägen 18, SE 75128 Uppsala, Sweden

ARTICLE INFO

Article history:

Received 16 November 2015

Received in revised form 17 February 2016

Accepted 11 April 2016

Available online 29 April 2016

Keywords:

Quick clay

Landslide

Radio-magnetotelluric

Seismic

Tomography

Coarse grain

ABSTRACT

Landslides attributed to quick clays have not only considerable influences on surface geomorphology, they have caused delays in transportation systems, environmental problems and human fatalities, especially in Scandinavia and North America. If the subsurface distributions of quick clays are known, potential damages can be mitigated and the triggers of landslides can better be studied and understood. For this purpose, new radio-magnetotelluric (RMT) and seismic data were acquired in an area near the Göta River in southwest Sweden that contains quick clays and associated landslides. High-resolution data along 4 new lines, in total 3.8 km long, were acquired and merged with earlier acquired data from the site. Velocity and resistivity models derived from first breaks and RMT data were used to delineate subsurface geology, in particular the bedrock surface and coarse-grained materials that overlay the bedrock. The latter often are found underlying quick clays at the site. Comparably high-resistivity and sometimes high-velocity regions within marine clays are attributed to a combination of leached salt from marine clays or potential quick clays and coarse-grained materials. The resistivity and tomographic velocity models suggest a much larger role of the coarse-grained materials at the site than previously thought, but they also suggest two different scenarios for triggering quick-clay landslides at the site. These scenarios are related to the erosion of the riverbank, increased pore-pressure and surface topography when close to the river and human activity when away from the river and where bowl-shaped bedrock surrounds the sediments.

© 2016 Elsevier B.V. All rights reserved.

1. Introduction

Landslides are natural geohazards that occur all over the world (Fig. 1). They claim hundreds of lives and damage infrastructure every year and may also cause environmental problems (GregerSEN and Løken, 1979; AB Svensk Filmindustri, 1957). They are a natural part of landform development (Crozier, 2010) and studies of landslides and areas prone to them are therefore important both to understand the current shape of the landscape and to avoid predictable financial damage and human loss of life, with implications for infrastructure designs and geological storage.

A landslide is generally defined as the movement of rock, debris and soil driven by gravity and preconditioned by the landform (Highland and Bobrowsky, 2008). Landslides can be classified into different categories depending on the types of materials (earth, rocks and debris) involved and the types of movements (fall, topple, slide, spread and flow); for example, rock fall and earth flow (Highland and Bobrowsky, 2008). Landslide triggering mechanisms are varied; they either have a single trigger or multiple sources; a combination of water saturation, seismic,

volcanic and even human activities. Examples of human activities triggering landslides are known in Sweden and Norway (Nadim et al., 2008; GregerSEN, 1981; Fig. 1b). Steepness of slope, morphology, soil type and underlying geology are the most important factors for causing landslides (Highland and Bobrowsky, 2008). Some of these factors are easier to study while others may not be, particularly due to inaccessibility. Subsurface geology is among those factors that cannot easily be studied or when studied the density of geotechnical boreholes used for this purpose is limited.

Quick-clay landslides, which are classified as earth flows (e.g., Torrance, 2014), are one of the most important geohazards in Northern countries including Sweden (Fig. 1), Norway, Japan and Canada (Geertsema and Torrance, 2005; Torrance, 2012). A small initial slip of quick clay may develop into large landslides that cover a vast area (Rankka et al., 2004) and as a consequence significantly change the terrain shape. Quick-clay landslides in Sweden mostly occur on relatively gentle topographic slopes made up of glacial and post-glacial sediments (e.g., silt and clay) and often bordered by open water such as a river or a lake (Nadim et al., 2008) similar to the example shown in Fig. 1d. For these types of landslides, which are often retrogressive, soil type and underlying geology are more important than the surface topography and morphology and, therefore these factors should be studied together.

E-mail addresses: shunguo.wang@geo.uu.se (S. Wang), alireza.malehmir@geo.uu.se (A. Malehmir), mehdad.bastani@sgu.se (M. Bastani).



Fig. 1. Example figures showing major quick-clay landslides and their impacts. (a) Tuve landslide, Sweden in 1977 and (b) Smårdö landslide, Sweden in 2006 (courtesy of the Swedish Accident Investigation Authority, SHK). (c) Lyngseidet landslide, Norway in 2010; it was likely triggered by loading of materials next to the shoreline (courtesy of the Geological Survey of Norway, NGU, photo: Andrea Taurisano, NVE). (d) Frästad landslide in our study area next to the Göta River (photo by Alireza Malehmir, 2011).

Based on known sites of quick-clay landslides, geotechnical (and/or geochemical) investigations and assessments have been implemented to understand quick-clay properties (e.g., Gregersen, 1981; Andersson-Sköld et al., 2005a; Geertsema and Torrance, 2005). However, due to the cost-effectiveness and ability to cover a large area and depth, a combination of geotechnical methods (e.g., cone penetration test) and surface geophysical methods is more desirable and has been more or less successfully used to study quick clays and their host environments (Rankka et al., 2004; Andersson-Sköld et al., 2005a; Löfroth et al., 2011; Bazin and Pfaffhuber, 2013; Malehmir et al., 2013a, 2013b; Dahlin et al., 2013; Adamczyk et al., 2013, 2014; Pfaffhuber et al., 2014; Lundberg et al., 2014; Shan et al., 2014; Salas-Romero et al., 2015; Helle et al., 2015; Shan et al., 2016). In this study we use a combination of electromagnetic and seismic methods and focus on an area near the Göta River in southwest Sweden in which quick-clay landslides have occurred (Fig. 1d).

This study complements to an earlier field campaign in year 2011 that covered part of the study area south of the Göta River. It is mainly based on new surface geophysical data acquired in year 2013 to extend some of the earlier geophysical profiles north of the river and west of the study area where a large portion of the area appears to be creeping towards the river (Fig. 2). The 2013 geophysical campaign focused on two geophysical methods that earlier studies have proved to be optimal for the study area, namely seismic and RMT methods (Malehmir et al., 2013a, 2013b). Results from the previous studies have revealed the surface of crystalline bedrock (20–100 m deep) dipping towards the river and layered glacial sediments, including coarse-grained materials (mostly sand) that sandwiched layers of quick clays, requiring a combined use of these methods for their delineation.

The main objectives of our study were (1) to expand our understanding of quick-clay distributions west and north of the area studied earlier and (2) to provide subsurface information about the general

structures at the site and evaluate quick-clay landslide potential at various parts of the study area. Given the increased length and area covered by the new geophysical data, the interpretations provided in this study are better constrained near the Göta River where the risk of quick-clay landslides is probably much higher due to the erosion of the foot of the slope (riverbank) and reduction of the lateral support.

2. Quick clays and their formations

Quick clay is defined as a clay with remolded shear strength less than 0.4 and 0.5 kN/m² (by fall cone test) and high sensitivity larger than 50 and 30, respectively in Sweden and Norway (Rankka et al., 2004; Donohue et al., 2012). The sensitivity is defined as the ratio between undrained, undisturbed shear strength and the remolded shear strength (Solberg, 2007; Shan et al., 2014). Undisturbed quick clay resembles a water-saturated gel that has formed through flocculation and deposition (Rankka et al., 2004) during and after the last glacial period. Undisturbed shear strength of quick clay is not different from non-quick clay, in other words the in-situ mechanical behavior is the same.

During the last deglaciation, about 11,000 years ago, meltwater from the Fennoscandian ice sheet and its receding glaciers carried suspended materials into marine or brackish waters where clays were deposited. Isostatic land uplift subsequently caused these marine clays to be raised above the sea level and exposed to fresh water infiltration (Brand and Brenner, 1981). Because of this, salt (saline) in the pores of marine clays have been leached out by infiltration of fresh/rain water or through fissures and fractures circulating fresh water from the bedrock (Malehmir et al., 2013a, 2013b; Shan et al., 2014). As a consequence, the bonds between adjacent clay particles become weaker and make the clay sensitive to mechanical disturbance and subject to ‘quickness’ (Rankka et al., 2004; Torrance, 2012). The reduction in the salt content and change in the structures of the clay imply higher electrical

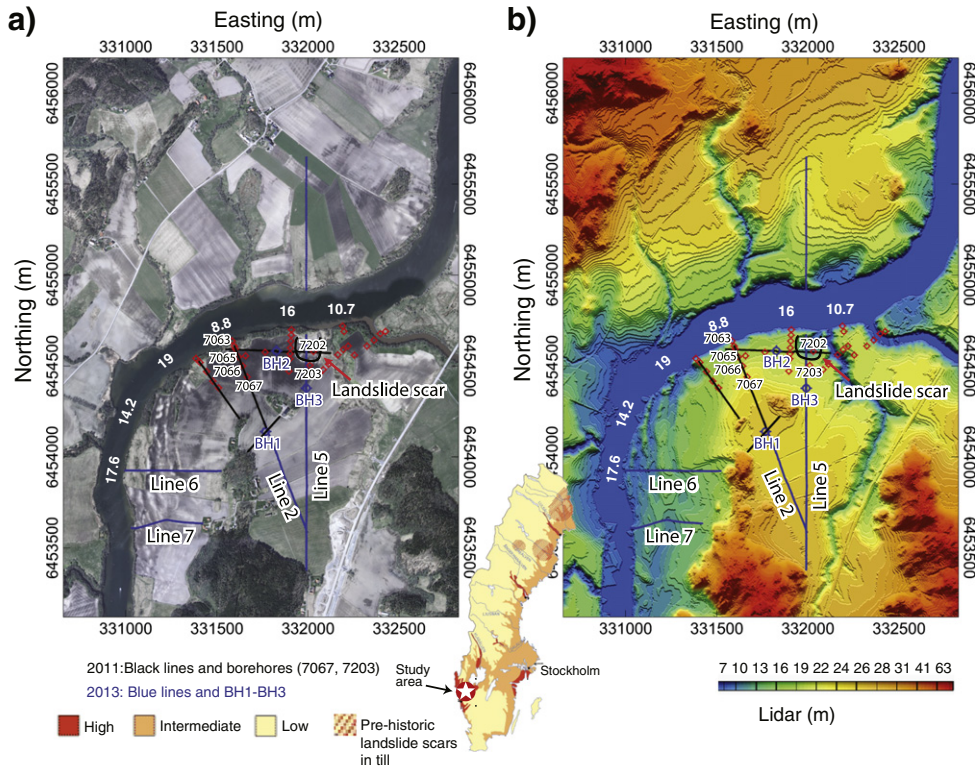


Fig. 2. (a) Aerial photograph and (b) LiDAR map showing the locations of the geophysical lines and major morphological features in the study area (modified from Malehmir et al., 2013a). Black lines are surveys carried out during 2011 and blue lines surveys (only seismics and RMT) carried during 2013 and presented in this study. Black curve represents the edge of a landslide scar, which is marked by a red arrow. Blue circles represent boreholes drilled as a follow up for the 2011 geophysical measurements. Red circles are geotechnical boreholes made available by the Swedish Geotechnical Institute (SGI), prior to 2011. Water depth is also marked by white color numbers.

resistivity when compared to the original marine clay. Quick clay shows much reduced remolded shear and bulk modulus (Rankka et al., 2004). Because of their high sensitivity, quick clay can liquefy by a sudden change in stress caused by, for example, uploading or unloading pressure. It has been suggested that even stress changes as small as the touch of a human hand can liquefy a laboratory sample of quick clay. However, for large deposits greater stress changes, such as increased saturation by excess rainwater, are required (Malehmir et al., 2013b).

3. Geophysical methods used for quick clay studies

Due to the relatively higher resistivity of quick clays compared to the surrounding marine clays, electrical resistivity tomography (ERT) has effectively been used to delineate their presence and extent (Rankka et al., 2004; Solberg, 2007; Solberg et al., 2012; Lundström et al., 2009; Löfroth et al., 2011; Donohue et al., 2012; Hibert et al., 2012; Long et al., 2012; Dahlin et al., 2013; Bazin and Pfaffhuber, 2013; Sauvin et al., 2014; Persson et al., 2014; Shan et al., 2014, 2016). Typically resistivities ranging between 10 and 100 Ωm have been used as a proxy for quick clays and resistivities below 10 Ωm for marine clays (Solberg et al., 2012; Long et al., 2012; Kalscheuer et al., 2013; Shan et al., 2014). While ERT is especially useful in delineating high resistivity features (Kalscheuer et al., 2013), it has a number of drawbacks that make the method occasionally unfavorable for quick clay studies. For example, penetration depth of ERT at the profile ends is limited, however, RMT is free from this problem.

Electromagnetic (EM) methods and their combination with ERT can be more useful to delineate quick clays mainly because the EM methods are more suited in resolving low-resistivity structures (Kalscheuer et al., 2013; Shan et al., 2014, 2016). However, such integrated use (Pfaffhuber et al., 2010; Shan et al., 2014, 2016) and joint inversion (Kalscheuer et al., 2008) are all related to a single physical property, namely the

resistivity; the diffusion phenomenon restricts the resolution of these methods (Bastani et al., 2012). Additionally, resistivity of quick clay also varies from one geological environment to another (Rømoen et al., 2010; Solberg et al., 2012). Therefore it is generally not easy to identify the soil types based on resistivity data alone (Rømoen et al., 2010). To reduce this problem, seismic methods have been used (e.g., Malehmir et al., 2013b; Lundberg et al., 2014; Adamczyk et al., 2013, 2014). By combining resistivity- and velocity-based methods, a multi-property (resistivity and velocity) model can be obtained and used to delineate quick clays and their host environment more accurately (Donohue et al., 2012; Hibert et al., 2012; Malehmir et al., 2013a; Sauvin et al., 2014; Persson et al., 2014).

4. Study area and available data

Our study area is situated near the Göta River (Figs. 1d, 2), north of the municipality of Lilla Edet in Sweden. Landslides near the Göta River have been catastrophic (e.g., Lilla Edet in 1957, AB Svensk Filmindustri, 1957), damming the river for a short period of time and contaminating the water by industrial chemicals moved in the water during the slide. The Göta River is the source of drinking water for more than 700,000 people with its surrounding areas that are largely industrialized. Quaternary deposits in the southern margin of the river are dominated by glacial tills. According to the LiDAR (light detection and ranging) elevation data (Fig. 2b), the surveying lines have few topographic variations; highland areas are primarily associated with shallow or exposed crystalline bedrock of granite and granodiorite. Coarse-grained materials (mainly sand), sometimes well sorted beach sand, and silty materials are often found within clayey materials sometimes at distinct intervals (Salas-Romero et al., 2015). A quick-clay landslide scar, 30–40 years old, with a typical retrogressive shape is present in our study area (Figs. 1d, 2b). It has been speculated that the base of

the slide (the slip surface) consists of coarse-grained materials (Malehmir et al., 2013a), implying that coarse-grained materials play an important role in controlling the size and extent of any potential quick-clay landslide at the site. The pore water pressure in the area is generally lower than hydrostatic pressure indicating downward ground water movements (Dahlin et al., 2013) but this may not be the case when the bedrock is close to the surface. Three cored boreholes in the sediments (BH1–BH3, Fig. 2), samples from them and downhole logging measurements (Salas-Romero et al., 2015) suggested the presence of coarse-grained materials (of various thickness, 10–30 m) underlying quick clays. Depth to bedrock was found to be at about 80 m close to the river and at shallower depths towards the south. Both quick clays and coarse-grained materials showed considerably low strength while marine clays, especially if rich in organic matter, showed high strength (Löfroth et al., 2011; Salas-Romero et al., 2015). Downhole velocity measurements were not successful because of polyvinyl chloride (PVC) casing. Only at locations where the casing was perforated (mainly to let fluids enter the drill hole) was a velocity around 1000 m/s observed. The PVC casing showed a velocity of about 1700 m/s implying that materials around the holes should in general have lower velocities than this (Salas-Romero et al., 2015).

At our study area, an extensive geophysical campaign was conducted in 2011 (Malehmir et al., 2013a) close to a series of geotechnical boreholes (Fig. 2; Löfroth et al., 2011). The study included a number of geophysical methods namely ERT, RMT, GPR, gravity and magnetics as well as P- and S-wave refraction and reflection seismics (Krawczyk et al., 2013). This was the first time that seismic methods were used for studying quick clays and their host environment in Sweden. The application of the seismic methods was helpful since bedrock and its undulations as well as the key coarse-grained layers underlying quick clays were accurately delineated through 2D and 3D refraction and reflection data imaging (Malehmir et al., 2013b; Lundberg et al., 2014; Adamczyk et al., 2013, 2014; Salas-Romero et al., 2015). A large number of surface materials with creeping properties located southeast of the study area (Fig. 2a) was not carefully studied nor understood if, for example, it was related to underlying quick clays or simply due to erosion from the river. It was important that the role of the river in the study area is better understood, thus justifying additional geophysical data further to the south and north of the river; earlier lines 2 and 5 were extended and new lines 6 and 7 were acquired (Fig. 2).

Table 1 summarizes the main parameters used to acquire the RMT data in this study. Ten meter station spacing was used along all the lines and more than 20 transmitters (14–250 kHz, with 10 dB S/N ratio) could be detected during the data acquisition. EnviroMT system of Uppsala University (Bastani, 2001) was used for this purpose. The RMT data are typically of good to excellent quality but occasionally noisy. As an example raw resistivity and phase data from line 2 are shown in Fig. 3.

Table 2 summarizes the main parameters used to acquire the seismic data. A receiver spacing of 4 m (10 m for wireless recorders) and shot spacing of 4 to 20 m was used. A Sercel 428 recording system with a maximum number of 400 channels (and 28 Hz geophones) was used for the recording. To cover the northern part of the study area on the other side of the river, we used 52 single-component wireless recorders connected to 10 Hz geophones and 24 three-component receivers

connected to MEMs-based (micro electro-mechanical system) sensors (Malehmir et al., 2016; Brodic et al., 2015). This means that for the acquisition of line 5 only, we deployed 398 receivers giving a total length of about 2250 m (Fig. 2). Except for line 5 where 20–100 g of dynamite were used (fired in hand-made holes of 0.5–1 m deep), data along other lines were acquired using a combination of an ESS100 accelerated weight drop (Malehmir et al., 2015) and a 5-kg sledgehammer. When the latter sources were used, 3–5 shot records were generated at every shot location and vertically stacked to improve the quality of the record. When explosives were used as the seismic source, the shot interval was increased from 4 m to 20 m. Fig. 4 shows example shot gathers from lines 2, 5 and 7. First arrivals and later events are clear on all these lines and particularly noticeable on line 5 data although the Göta River runs in the middle of the line (Fig. 4c). Clear refracted arrivals and indications of dipping bedrock can already be seen in some of the shot gathers (Fig. 4b).

Seismic and RMT data from the two campaigns (2011 and 2013) were then merged and used in this study. No focus has so far been given to the reflection component of the new acquisition campaign and thus the new reflection seismic data are not presented here but will be the focus of our future studies. The main focus has therefore been on first break tomography and RMT data inversion from the combined data sets and comparison with the reflection results obtained during the 2011 survey and available geotechnical information and the three boreholes drilled in the study area.

5. Methods and their basis

5.1. RMT method and inversion

RMT is a passive-source electromagnetic method where the signal sources are distant radio transmitters that operate in the frequency range 14 to 250 kHz. Usually the radio transmitters are located far away from the survey area so that a plane-wave assumption for the EM signals is valid, and allows the estimation of electrical resistivity (Tezkan et al., 1996; Bastani, 2001; Pedersen et al., 2006; Bastani et al., 2012). RMT data acquisition consists of measuring three components of the magnetic field (H_x , H_y and H_z) and two horizontal components of the electric field (E_x and E_y). The electric and magnetic field components are related through the impedance tensor Z , which in the frequency domain is given as:

$$\begin{bmatrix} E_x \\ E_y \end{bmatrix} = \begin{bmatrix} Z_{xx} & Z_{xy} \\ Z_{yx} & Z_{yy} \end{bmatrix} \begin{bmatrix} H_x \\ H_y \end{bmatrix} \quad (1)$$

where x and y represent the measurement directions in Cartesian coordinate system. Z_{xx} , Z_{xy} , Z_{yx} and Z_{yy} contain information about resistivity of the subsurface structures.

Apparent resistivity at the surface of the Earth is defined as (Bastani, 2001):

$$\rho_a = \frac{1}{\mu_0 \omega} |Z_{yx}(\omega)|^2 = \frac{1}{\mu_0 \omega} \left| \frac{E_y(\omega)}{H_x(\omega)} \right|^2 \quad (2)$$

and the phase of the impedance is given by:

$$\phi(\omega) = \tan^{-1} \left[\frac{\text{Im}(Z_{yx})}{\text{Re}(Z_{yx})} \right], \quad (3)$$

where μ_0 is the permeability of free space and ω is angular frequency.

The determinant of the impedance tensor is defined as:

$$Z_{\det} = \sqrt{Z_{xx}Z_{yy} - Z_{xy}Z_{yx}}. \quad (4)$$

Table 1
Main RMT data acquisition parameters, 2013.

Survey parameters	Line 2	Line 5 ¹	Line 5N ²	Line 7
Recording system	EnviroMT	EnviroMT	EnviroMT	EnviroMT
No. of stations	43	128	31	48
No. of transmitters	>20	>20	>20	>20
Station interval (m)	10	10	10	10

¹: line 5 southern side of the river; ²: line 5 northern side of the river.

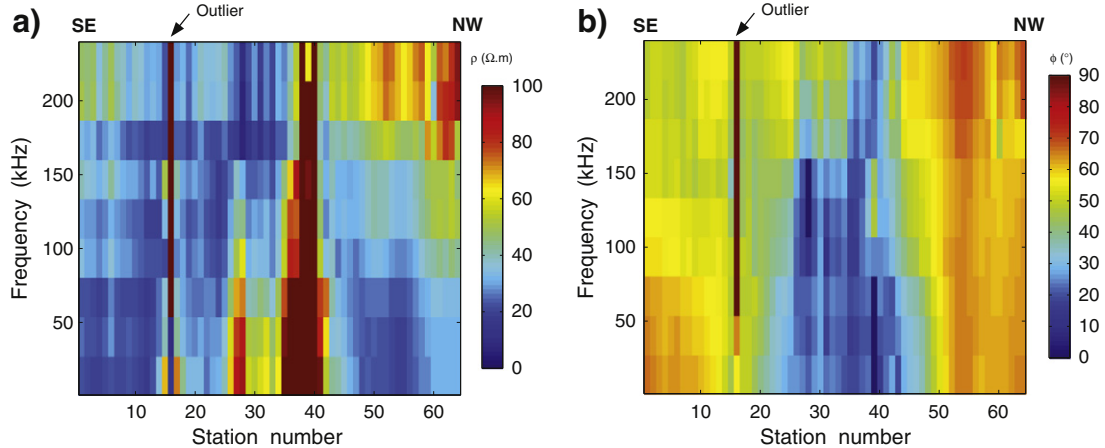


Fig. 3. Example (a) apparent resistivity and (b) phase data from the RMT measurements along line 2 showing their quality with a few outliers that were excluded from the inversion.

Based on the study conducted by [Pedersen and Engels \(2005\)](#), 2D inversion of the determinant data is more preferable than 2D transverse electric (TE) and transverse magnetic (TM) model inversions when the resistivity distribution is considered 3D. Following their recommendations, we also used the determinant data to carry out 2D inversions of the RMT data collected at the site.

Prior to the RMT inversion, a careful inspection of the data was carried out. Outliers or noisy data ([Fig. 3](#)) were removed on the assumption that EM data should be essentially smooth due to the diffusion process in the earth ([Nabighian, 1987](#)). During the inversion we applied an error floor to down-weight the data with unrealistically small errors ([Bastani et al., 2012](#)). For the inversion, we used the EMILIA program, which is a modified version of REBOCC program ([Siripunvaraporn and Egbert, 2000](#)) developed by [Kalscheuer et al. \(2008\)](#). The forward operator is based on a finite-difference algorithm ([Kalscheuer et al., 2008; Siripunvaraporn and Egbert, 2000](#)). Damped-OCCAM was the inversion strategy. It introduces smoothness constraints in both horizontal and vertical directions ([Constable et al., 1987](#)) to stabilize the inversion, which allows it to converge faster. A 100 Ωm half-space was used as the inversion-starting model. Model parameterization was done with different strategies for the horizontal and vertical directions. In the horizontal direction, 5 m cells were used in the middle zone of the model, then expanded to several hundreds of meters towards the later sides to achieve boundary condition. In the vertical direction, cells had

0.5 m size at the surface and increased logarithmically with depth (for example 200 m at about 600 m depth).

5.2. Seismic methods and first break tomography

P-wave reflection and refraction are the main methods used in the seismic surveys. For the reflection data, we used the results reported by [Malehmir et al. \(2013b\)](#) meaning that only portions of the seismic lines 2 and 5 have reflection seismic sections to compare with our new results. Detailed description of the reflection data processing can be found in [Malehmir et al. \(2013b\)](#). It follows a standard pre-stack data enhancement and post-stack migration algorithm with a special focus given to refraction static corrections and velocity analysis. The processing was successful in that it revealed at least two sets of reflections (at around 20 and 35 m depths) above dipping bedrock and overlapping it.

For this study, we combined the raw data from the 2011 survey that cover only parts of lines 2 and 5 (see also [Adamczyk et al., 2013, 2014](#)) and combined them with the new data from 2013. After setting up the geometry for the merged data, we picked the first arrivals automatically and corrected them manually when required. First breaks are mostly of good quality ([Fig. 4](#)) but at places close to the highway in the southern end of lines 2 and 5 coherent surface-wave noise occasionally made it difficult to pick the first breaks even after the vertical stacking of the repeated shot records (e.g., [Fig. 4a](#)). From the study of the reciprocity times, we estimated the error in the picking of the first breaks to be on the order of 2–3 ms. No need to correct the data phase and amplitude of the MEMs sensors (accelerometer) was required in contrast with the geophones (velocity meter) as we only used them for refraction data analysis ([Brodic et al., 2015](#)). This is clearly noticeable from the first breaks of the shot gather shown in [Fig. 4c](#); mixed geophones and MEMs are used on the other side of the river. [Fig. 5a](#) shows first break picks as a function of offset for the data along line 5 clearly showing low velocity materials (glacial sediments) above a high velocity zone (bedrock). First breaks up to 1800 m offset are available from this line implying a deep penetration is possible using refracted component of the data.

First, we carried out refraction data analysis but we subsequently decided to focus on first break tomography to fully account for crookedness of the lines. The PS_tomo ([Tryggvason et al., 2002](#)) 3D first break tomography was used for this purpose. The algorithm is based on [Benz et al.'s \(1996\)](#) ray-tracing method but uses a finite-difference forward modeler to calculate the first breaks for all the shot and receiver combinations ([Podvin and Lecomte, 1991; Hole and Zelt, 1995](#)). A LSQR conjugate gradient solver ([Paige and Saunders, 1982](#)) is then used to modify velocity model information. The inversion starts with a

Table 2

Main seismic data acquisition parameters of the 2013 survey. The 2011 seismic data acquisition parameters can be found in [Malehmir et al. \(2013b\)](#).

Survey parameters	Line 2	Line 5	Line 6	Line 7
Recording system	SERCEL 428	SERCEL 428	SERCEL 428	SERCEL 428
No. of receivers	160	398	133	100
No. of shots	157	87	130	100
Receiver interval (m)	4	4/10	4	4
Shot interval (m)	4	20	4	4
Maximum offset (m)	640	2247	528	396
Source type	WD ¹	Ex ²	WD ¹ /H ³	H ³
Charge size (gr)	50–200			
Recording parameters				
Record length (s)	6	10	10	10
Sampling rate (ms)	0.5	0.5	0.5	0.5
Geophone frequency (Hz)	28	28/10/MEMs	28	28
No. of geophones per set	Single	Single	Single	Single
No. of shots/point	5	1	5	3–5
Shot depth (m)	0	0.5–1	0	0

1: weight-drop; 2: explosive; 3: hammer.

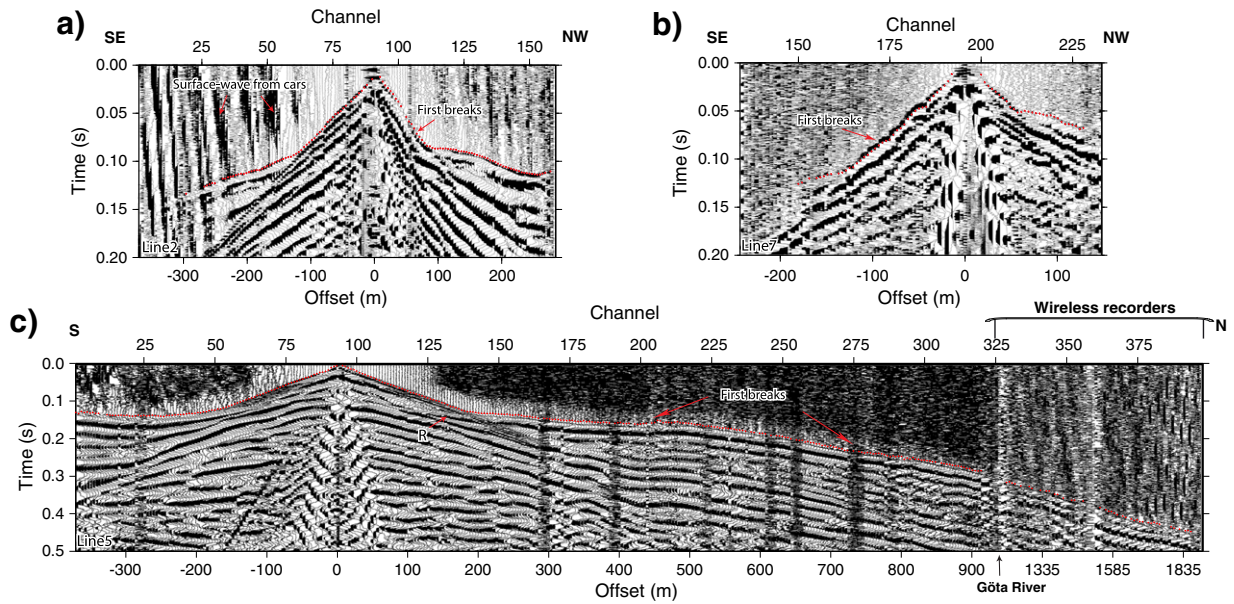


Fig. 4. Example shot gathers (after vertical stacking of repeated shot records) from (a) line 2, (b) line 7 and (c) line 5 (Fig. 2). Note that the quality of the first breaks (red dots) is particularly good for the data along line 5 where explosives were used as the seismic source. Göta River runs in the middle of the line hence wireless recorders were used on the northern side of the river. Note also that southern side of line 2 is near a major highway influencing the data (even after vertical staking of the repeated shots) by coherent surface waves. There are also indications of shallow reflections (R) in the data illustrating the quality of the seismic data.

initial model, which honors the topography information; topography should be used and cells above this will have velocities of air (e.g., 340 m/s). Regularization is done during various stages of the inversion. To partly constrain the inversion, we used near-offset travel times to produce a starting model for the inversion. Although the inversion is done in 3D, we used three cells in the lateral directions and made the

cells large enough so that most rays stay within the middle cell. This would then allow presenting the data as 2D section (a slice through the 3D model) although all the calculations are done in 3D. Along the line we used 4 m cell size in the horizontal direction and 2 m in vertical direction. In total 9 iterations of inversions were performed and the most plausible velocity model with the least RMS error (often one of

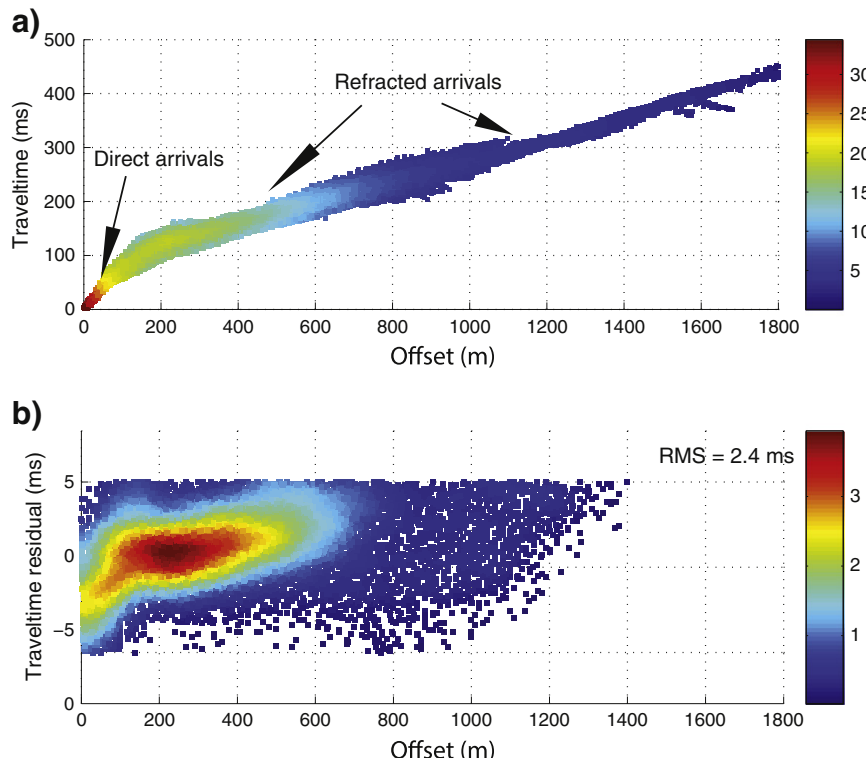


Fig. 5. Example (a) first breaks used for tomography and (b) residual times (observed minus forward calculated) obtained from the tomography model used to present the results from line 5. Color bar shows the point density. Clear indication of the bedrock is noticeable in the first breaks.

the last iterations) was chosen for the interpretations. Fig. 5b shows example RMS errors (forward minus observed first breaks) as a function of offset indicating a good fit for the model obtained along line 5.

6. Results and interpretations

In the following subsections we present results from the inversions and comparisons between the geophysical and geotechnical data along individual lines (Fig. 2). We use the same distance along the lines to define the location of various data and for consistency in the presentation of the results.

6.1. Line 2

Line 2 is the second longest in the study area and ends close to the bank of the Götä River (Fig. 2). Borehole BH1 is at about 600 m distance along the line where the bedrock was reached at about 33 m depth. Just 100 m east of the borehole, bedrock is exposed suggesting an undulating bedrock surface in this part of the line. In addition to this borehole, we also preset available geotechnical boreholes (Löfroth et al., 2011, Fig 6) where either they end at coarse-grained materials (or bedrock) or present the location of quick clays. Both RMT model and seismic tomography results suggest a bedrock depth of approximately 10 m north of BH1 (Figs. 7a, b). It is represented by high velocity and resistivity boundaries. Given the length of the line and the low velocity materials in the southeastern part of the line, tomography results have enabled imaging down to about 150 m depth, which provides valuable information. Bedrock depressions are quite visible in the tomography results and important when the risk of landslide is discussed. Bedrock dips towards the river as expected. An interesting zone of higher velocity (around 1700–2500 m/s) is observed in the tomography results, which corresponds well to places where coarse-grained materials were observed in BH1 (Fig. 7a). In the RMT data, this zone appears as a more resistive layer (Fig. 7b) and suggests that there may be quick-clay and fresh-water circulating within the coarse-grained materials. Fig. 7c illustrates the comparison between the models and borehole information (Salas-Romero et al., 2015). It is unlikely that the lower velocity region below the coarse-grained layer is not resolved by the tomography and only remained from the starting model (not updated from the starting model). The bedrock however is well resolved and this would then allow interpreting the whole tomography section. We

used the method by Spies (1989) to estimate the penetration depth of the RMT data shown as white dashed line (Fig. 7b). Features above the penetration depth in the model are resolved by the RMT data with a high confidence. This means that the bedrock and the coarse-grained layer interpreted from the data are well resolved and can be considered real.

For comparisons with the reflection results, we superimposed the tomography and RMT models onto them (Figs. 7d, e). There is a good correspondence among the RMT, tomography and reflection sections as well as available geotechnical boreholes further verifying our results.

6.2. Line 5

Line 5 is the longest (>2.2 km) in the study area and was designed to provide information about the depth to bedrock below the river (Fig. 2). Borehole BH3 and geotechnical boreholes (7202 and 7203 in Figs. 2, 8f) are located on/close to the line providing constraints for the interpretation of the results. RMT data have a gap at the river since no lake-RMT data acquisition was carried out (Bastani et al., 2015). However, because of the wireless seismic recorders and simultaneous recording of the seismic data, tomography results contain velocity information also under the river (Fig. 8a). Undulating bedrock is clearly seen and shows large depressions with the deepest point below the landslide scar at a depth of about 90 m. Between 900 m and 1700 m distance along the line bedrock reaches close to the surface allowing RMT signals to penetrate the sediments above the bedrock on the both sides of the river. It is evident that there are more sediments on the southern side of the river than on the northern side. The main quick-clay landslide is located on the southern side of the river, which may imply that there is larger erosion on the southern side of the river than on the northern side, although the level of water in the river primarily controls this. The unconsolidated sediments on top of the bedrock have a velocity less than 2000 m/s. RMT data also delineate the bedrock on the southern side of the river, but do not clearly depict its features and geometry deeper down (see in Fig. 8a) as observed in Fig. 8b. Interestingly, RMT data again resolves a thin relatively high resistivity zone above the bedrock (Fig. 8b) in accordance with the position of a major coarse-grained layer observed during the drilling of BH3. This layer overlaps the bedrock and is also observed as a slightly higher velocity zone and resistive zone than the bedrock on the northern side of the river. Careful

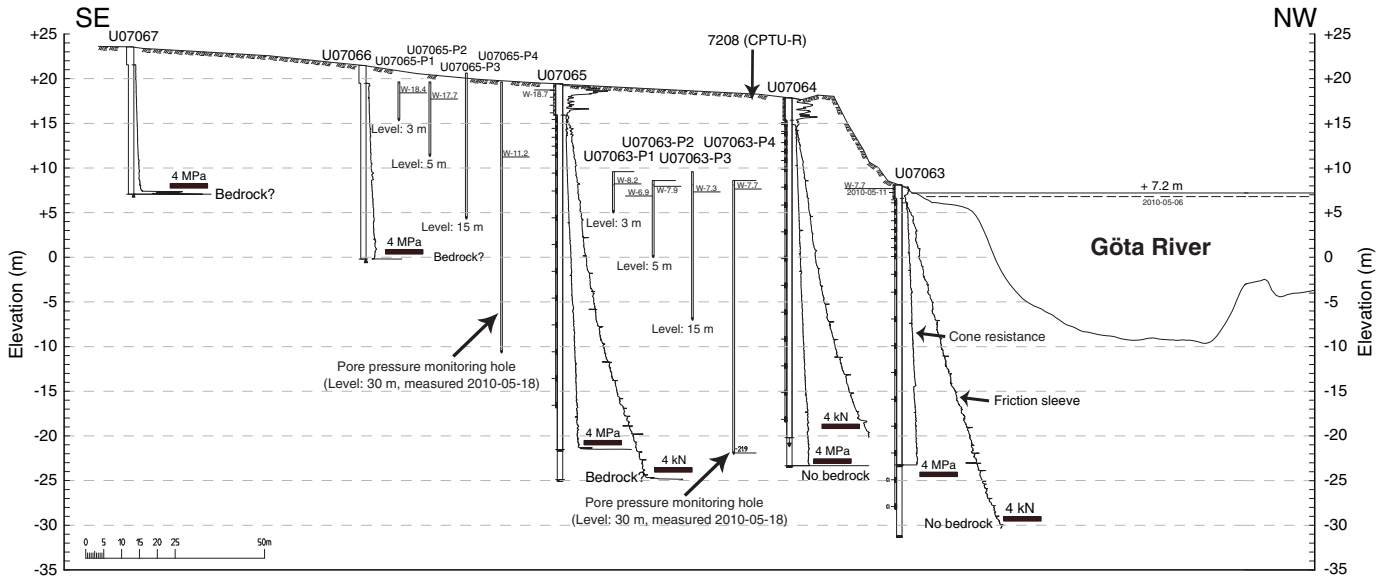


Fig. 6. Cross section almost parallel to parts of seismic line 5 showing CPTU measurements including cone resistance (shown in MPa) and sleeve friction (shown in kN) in the boreholes (Fig. 2). Borehole 7063 and 7065 were used for pore-pressure monitoring at four depth levels (P1–P4). Modified from Löfroth et al. (2011).

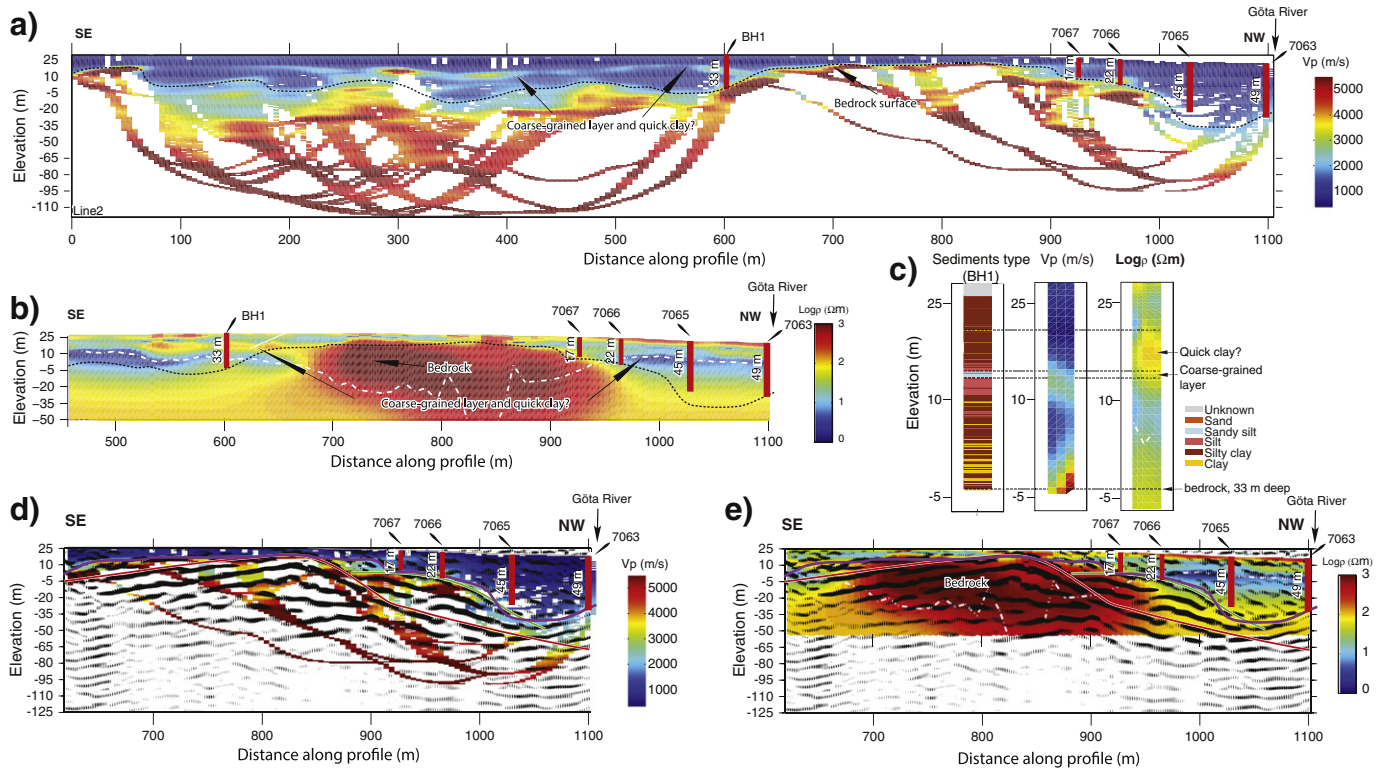


Fig. 7. (a) Tomography and (b) RMT models of line 2. (c) Correlation between borehole data (BH1) and the models close to the borehole. (d and e) Available reflection seismic data (from 2011) superimposed on the velocity and resistivity models, respectively. Same depth and distance scales are used in all the subfigures for comparison. RMS (root mean squared difference between observed data and modeling responses) of resistivity model is 1.8 and RMS (root mean squared time residual) of tomography is 2.2 ms. Geotechnical boreholes 7066 and 7067 (Löfroth et al., 2011) show good correlation with the reflection, resistivity and tomography results. Black dashed lines in (a) and (b) and violet lines in (d) and (e) represent bedrock surface obtained from tomography. The white dashed line in (b) and (e) represents penetration depth of the RMT data. Solid red and green lines in (d) and (e) represent the structure boundaries in bedrock obtained from reflection.

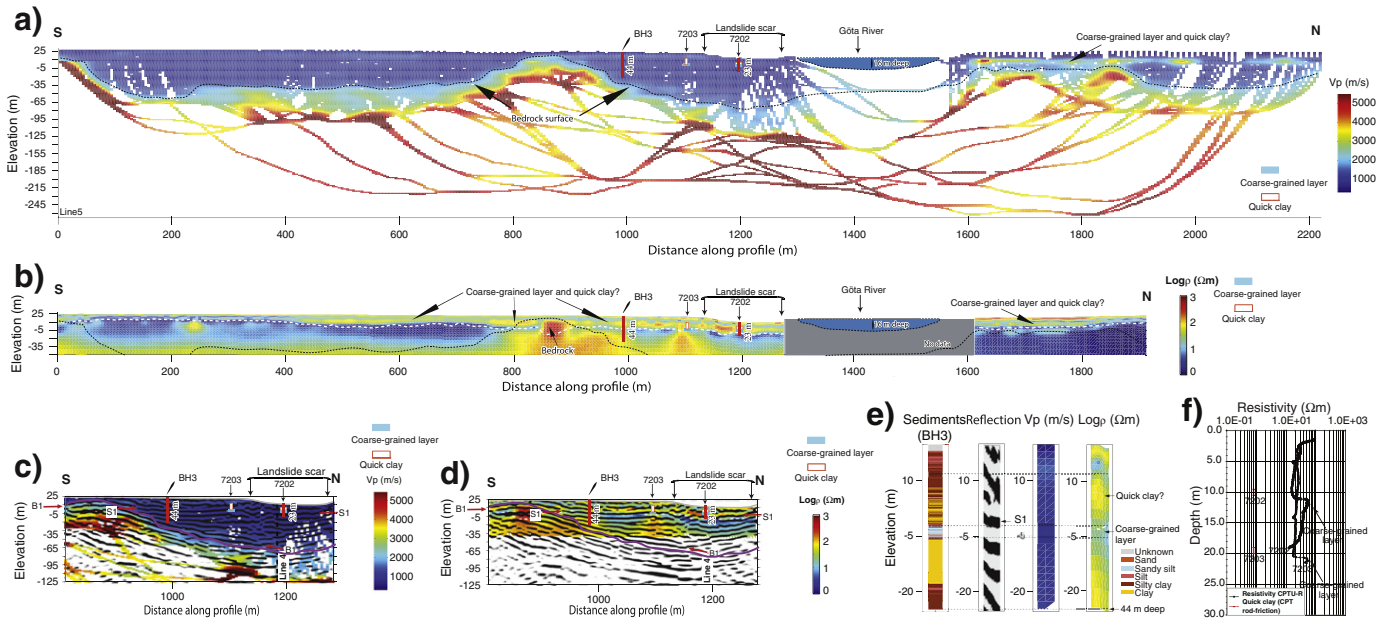


Fig. 8. (a) Tomography and (b) RMT models of line 5. (c and d) Available reflection seismic data (from 2011) superimposed on the velocity and resistivity models, respectively showing a good correspondence for many features in particular the bedrock at the shallow depths. (e) Correlation between borehole data (BH3), available reflection seismic and the inverted models at the same location. (f) Available geotechnical data (from 2011). The gray part in (b) means no RMT data due to the river. RMS of resistivity model is 2.1 and 1.4 for the southern and northern parts of the river, respectively and RMS of tomography is 2.4 ms. Black dashed lines in (a) and (b), violet lines in (c) and (d), and white dashed dot lines in (b) and (d) represent the same parameter as described in Fig. 6. In (c) and (d), S1 and B1 are interpreted as a coarse-grained layer and bedrock reflectors, respectively.

inspection of the RMT penetration depth again suggests that this feature is real and resolvable by the RMT data (see the white dashed line in Fig. 8b).

For comparisons with the reflection results, we have superimposed the tomography and RMT models onto the reflection seismic profile along line 5 (Figs. 8c, d). A reflection (marked as S1) at about 20 m depth overlapping the bedrock (B1, dipping towards the river) well matches the high-resistivity zone interpreted to be from a combination of the coarse-grained layer and possibly quick clays. Landslide mass resides on these materials (likely mainly silty-sandy today). It is evident that the tomography results this time are unable to resolve this feature but reflection and RMT data do. Comparison with the borehole results shown in Fig. 8e illustrates this. The sandy-silty layer corresponds to resistivities above 40 Ωm . Above this layer, even higher resistivity features show up, which probably indicate the presence of the quick clays (or silty clays) observed by Salas-Romero et al. (2015).

6.3. Line 6

Line 6 runs in east–west direction and was placed to check the peculiar surface topography pattern in the study area, which suggests a gradual movement of the materials towards the river (Fig. 2). Along this line only seismic data were collected and hence only tomography results are available. Bedrock is, however, exposed near the easternmost part of the line that can be used to validate the tomography results. The maximum depth of the velocity model is about 120 m due to the low velocity materials allowing deeper penetration (Fig. 9). Bedrock surface is again undulating but has a general dip towards the river. Similar to the results along line 2, there are indications of high velocity zones/layering within the clayey materials, which we think originate from coarse-grained sediments at various depth intervals but most importantly overlapping the bedrock. Reflection data by Malehmir et al. (2013b) and Lundberg et al. (2014) suggest at least two sets of coarse-grained materials within the clayey-silty sediments.

6.4. Line 7

Lines 6 and 7 are parallel and were planned for the same purpose as mentioned above. Cross-shooting did not result in any tomography information mainly because of the large distance between the two lines. Individual tomography results from this line, however, suggest similar features as those observed along line 6 (Fig. 10a). Bedrock is again exposed in the easternmost part of line 7 and this is nicely depicted by the RMT results (Fig. 10b). A dry crust is also observed in the RMT model originating from the creeping and small surface topography variation in that area (Fig. 2). It is remarkable again to observe a high resistivity (around 50 Ωm) zone above the bedrock and in particular at 150 to 350 m distance along the line. This high resistivity may suggest the presence of large pockets of quick clays and coarse-grained materials that contribute to the soil instability in this part of the study area. RMT data are unable to resolve the bedrock mainly due to the large amount of clays limiting their penetration depth.

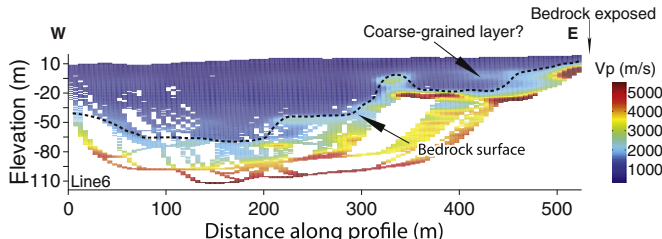


Fig. 9. Tomographic model of line 6 (RMS 2.2 ms). Bedrock is exposed at the eastern end of the line as clearly resolved by the tomographic model. There are also indications of high velocity materials inside the clayey setting suggesting possibility of coarse-grained materials (sometimes underlying quick-clays).

7. Discussion

7.1. Quick-clay and coarse-grained materials

Usually, the resistivity of quick clay varies from between 10 and 100 Ωm (Solberg et al., 2012; Long et al., 2012; Kalscheuer et al., 2013; Shan et al., 2016), which is significantly higher when compared to the surrounding marine clays (<10 Ωm). If clayey sediments have resistivity values in the range 10–100 Ωm and the surrounding materials are relatively conductive, those sediments have a possibility to contain quick clays. Malehmir et al. (2013a, 2013b) and Salas-Romero et al. (2015) have reported that the quick clays are often found directly above the coarse-grained materials, which have a strong seismic reflection character (Fig. 8e) and in some of our cases tomography character (Figs. 7a, 8a). Coarse-grained materials in the study site are mainly beach sands with even evidence of marine or brackish-water fossil shells (Salas-Romero et al., 2015) in them.

Combining all the above-mentioned features, we conclude that sedimentary units composed of both quick clays and coarse-grained materials together show relatively high velocity and high resistivity features when compared to marine clays. This is evident for the data along line 5 particularly at around 10–20 m depth at 1600–1900 m distance (Fig. 8, Löfroth et al. (2011) confirmed existence of quick clays at this specific site) and along line 7 at 10–30 m depth at 200–300 m distance (Fig. 10). All those special areas mentioned are close to the riverbank, which is usually one of the most suitable places for quick-clay landslides naturally triggered (Nadim et al., 2008).

To support the interpretation of the RMT data and given their limited penetration depth due to highly conductive marine clays in the area, we generated synthetic data from two models as shown in Fig. 11a and c. The inversions (Fig. 11b, d) of the synthetic data show that the RMT data are likely unable to distinguish between quick-clays and coarse-grained materials if they juxtapose and sandwich each other and the low resistivity marine clays. This arrangement also explains why resistivity measurements should always be supplemented by geotechnical investigations as suggested by Andersson-Sköld et al. (2005b). RMT data along line 7 at around 7–15 m depth at 160–300 m distance (Fig. 10) and line 5 at around 15 m depth at 200–1250 m distance (Fig. 8) show a relatively high resistivity layer, which may be an indication of quick clay if the resistivity range of quick clays are only considered. However, they are not necessarily of high sensitivity, which would need to be verified by geotechnical measurements.

7.2. Quick-clay landslides and role of subsurface geology

Quick-clay landslide probability is determined by topography, erosion potential and geotechnical properties. Subsurface geology also influences the probability and extent of a landslide. The new geophysical lines presented here provide a better understanding about the geological setting at the site, resolving bedrock at different parts and how this can have a control on the development of quick-clay landslide at the site. Fig. 12 shows the 3D visualization of the RMT and tomography models from all the new and merged lines. One obvious feature of the models is the dipping bedrock towards the Göta River from different directions with varying surface morphology. Fig. 13 shows a schematic cross section hypothesizing a scenario that can explain the formation of the quick clay and potential zones with high quick-clay landslide risk in the study area. We conclude that the mini-basin shape (Figs. 7a, 8a, 13) of the bedrock topography towards the southern side of the study area is an important feature. Its presence suggests that a quick-clay landslide will only be triggered if the supporting materials are removed (partly or completely) by human activity. Several documented quick-clay landslides have been associated with construction work (GregerSEN, 1981; Nadim et al., 2008). We anticipate that areas in bedrock depressions are at low risk of failure unless the environment is disturbed by other activities than natural ones (like road construction,

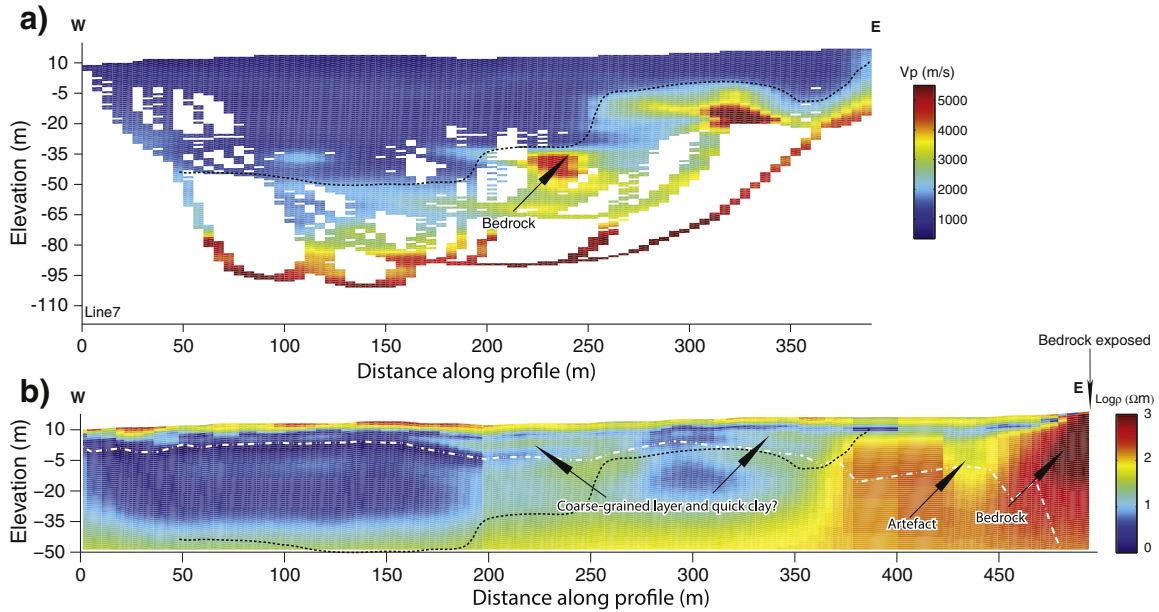


Fig. 10. (a) Tomography (RMS 2.2 ms) and (b) RMT (RMS 2.1) models of line 7. Bedrock is exposed on the easternmost part the line as well resolved by the RMT data. Seismic line was shorter than the RMT line in this case. Note high velocity and resistivity materials inside the clayey setting suggesting the possibility of coarse-grained and quick-clay materials. Bedrock is well resolved by the tomographic model as dipping towards the river.

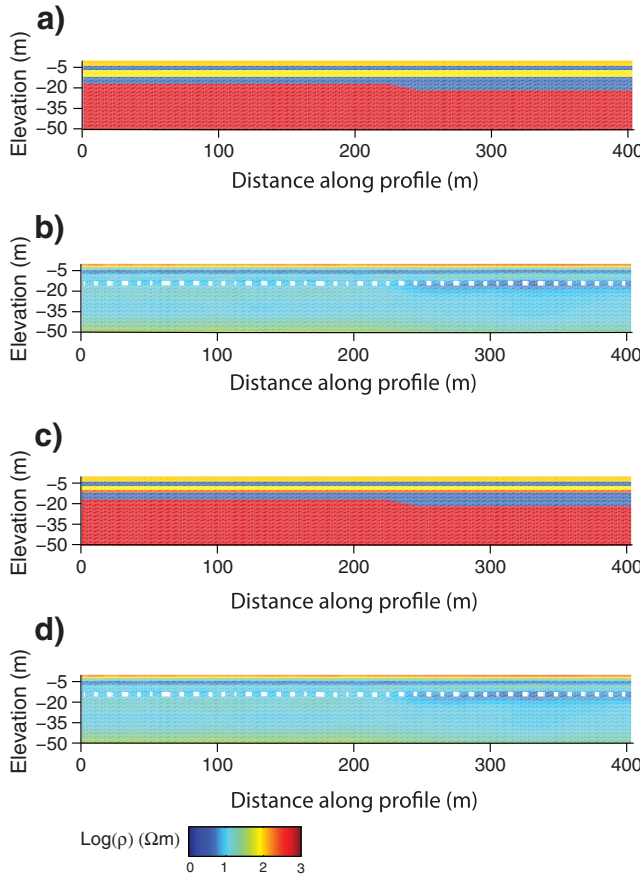


Fig. 11. (a and c) Synthetic models used to generate RMT data to test the possibility of resolving quick clay in the RMT data. We split the third layer in the model (a) into two layers in the model presented in (c). The third layer with $80 \Omega\text{m}$ resistivity represents quick clay in (a) and (c), and the fourth layer with $200 \Omega\text{m}$ resistivity in (c) represents coarse-grained materials. (b and d) Inverted models of the RMT data from the models (a) and (c), respectively. It is clear that both models have no significant differences. The high resistivity features in the real RMT models are caused by a combination of quick clay and coarse-grained materials as this synthetic data modeling suggests.

region A in Fig. 13). The situation is, however, different in areas close to the river where lateral erosion can play a main role (region B in Fig. 13). Sudden increases in pore pressure may trigger quick-clay landslide with the coarse-grained layer as the main slip surface. After the Tuve landslide in Göteborg in 1977 (which took 9 lives, destroyed 66 houses and made 600 people homeless), observers reported a large quantity of sand (Rudberg, 1997) in the area although there is no published account that describes the role of the sand in the slide. In both cases (A and B in Fig. 13), the presence and formation of quick clays are possible, but to what extent they exist needs to be investigated using for example drilling and sampling as performed by Löfroth et al. (2011) and Salas-Romero et al. (2015). The large amount of sediments observed at the southern side of the river (Fig. 13) may also imply that this region is susceptible to quick-clay landslides, but this needs to also be investigated further and ground water flow needs to be understood.

Salas-Romero et al. (2015) also reported the presence of biogenic gas at shallow levels (Fig. 13) during the drilling of BH2 immediately at the location of the coarse-grained layer. The gas leaked out because the impermeable clays above were penetrated by the drill hole. At greater depths, a few meters above the bedrock, organic-rich clays were observed. It is unclear what kind of interaction a quick-clay landslide and gas release would have: this has not been given any previous attention and is worth for future study.

The western side of the study area shows creeping soils on the aerial photograph (Fig. 12), which may be an important signal for slowly processing earth flow (Highland and Bobrowsky, 2008). RMT data from line 7 likely suggest downward water flow (infiltration, Dahlin et al., 2013) but also a possibility for the bedrock to act as a good surface for the groundwater flow (Fig. 13) to get directed into the coarse-grained layer forming quick clays (upward leaching in confined aquifers).

7.3. Possibility for joint inversion

Seismic refraction and tomography methods provided velocity and subsurface geometry information, especially about the bedrock and in this case also about key layers above the bedrock (e.g., coarse-grained layers). The RMT method provided detailed resistivity information close to surface but lacks resolution at depth. A combination of the methods, however, enabled us to overcome the shortcomings of each

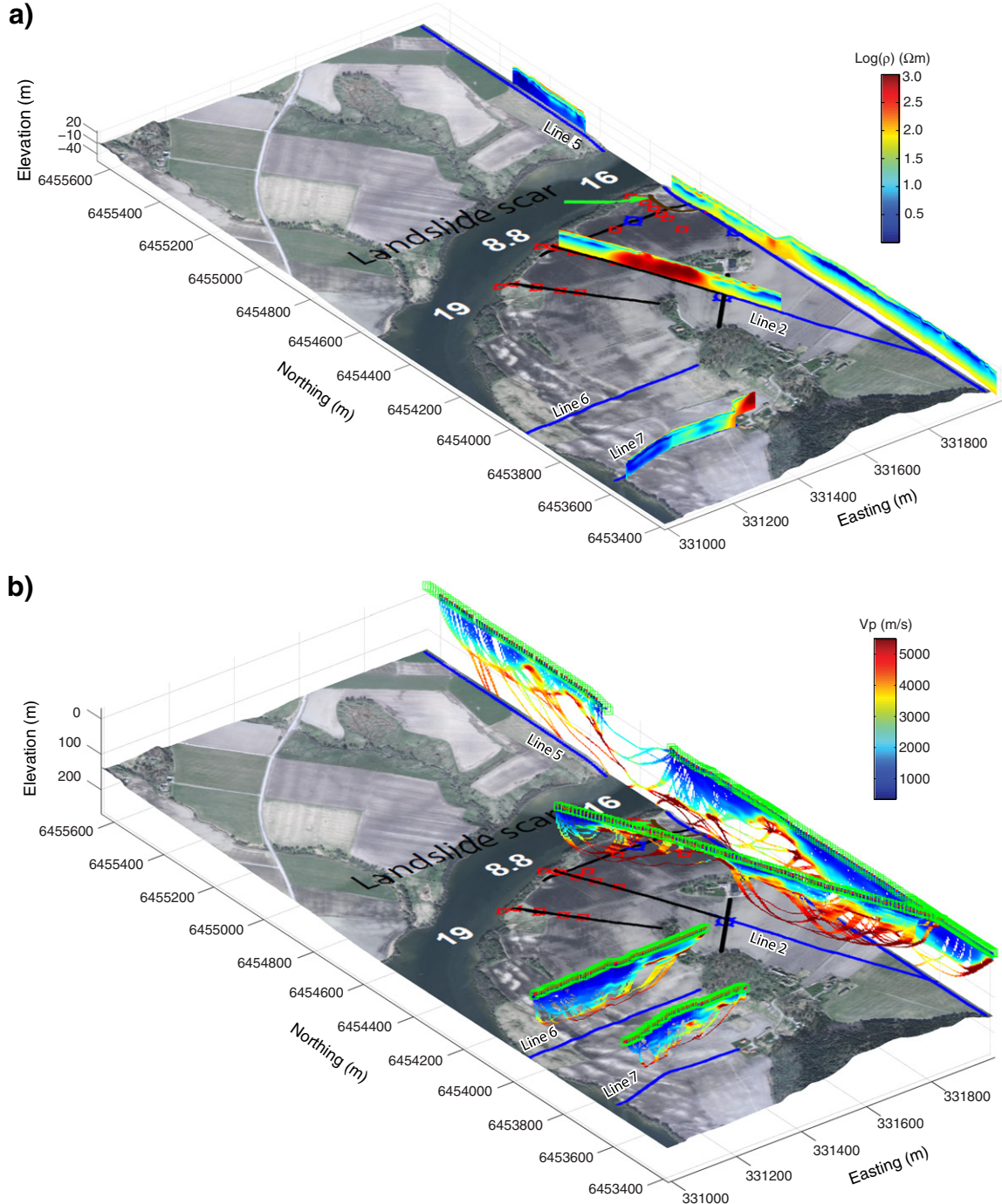


Fig. 12. 3D visualization of (a) resistivity and (b) velocity models along all the lines presented in this study. Base map is the aerial photograph superimposed onto the LiDAR surface of the study area. Elevation is reduced by 50 m in (a) and 180 m in (b) for display purposes.

method and also allowed us to better constrain the interpretation where comparable results were obtained. The boundaries between quick clays, coarse-grained materials and surrounding clays in the geophysical models are not as clear as in the geotechnical data, for several reasons. One reason is due to the smoothness constraint that is used to avoid instability of the inversions. Another reason to mention is the diffusive nature of these methods, which all suffer poorer resolution as depth increases. In our case study, it does not matter if quick-clay or coarse-grained layer is the target, they both have layered structures (although it may be pocketed or patchy at places). It may be possible to jointly invert (e.g., Moorkamp et al., 2013) for both resistivity and velocity models for certain lines. Since there is already a good correlation

between the two models (e.g., Figs. 7c, 8e), the chance that the joint inversion would be successful is highly likely.

8. Conclusions

We have employed RMT and seismic methods, and extended an earlier study on delineating subsurface geology of an area prone to quick-clay landslides in southwest Sweden. A long line crossing both the Göta River and a major landslide was designed to provide information about bedrock depth and undulations. Two lines were planned to study creeping of soils observed in the western part of the study area. Both resistivity and velocity models have in many places good

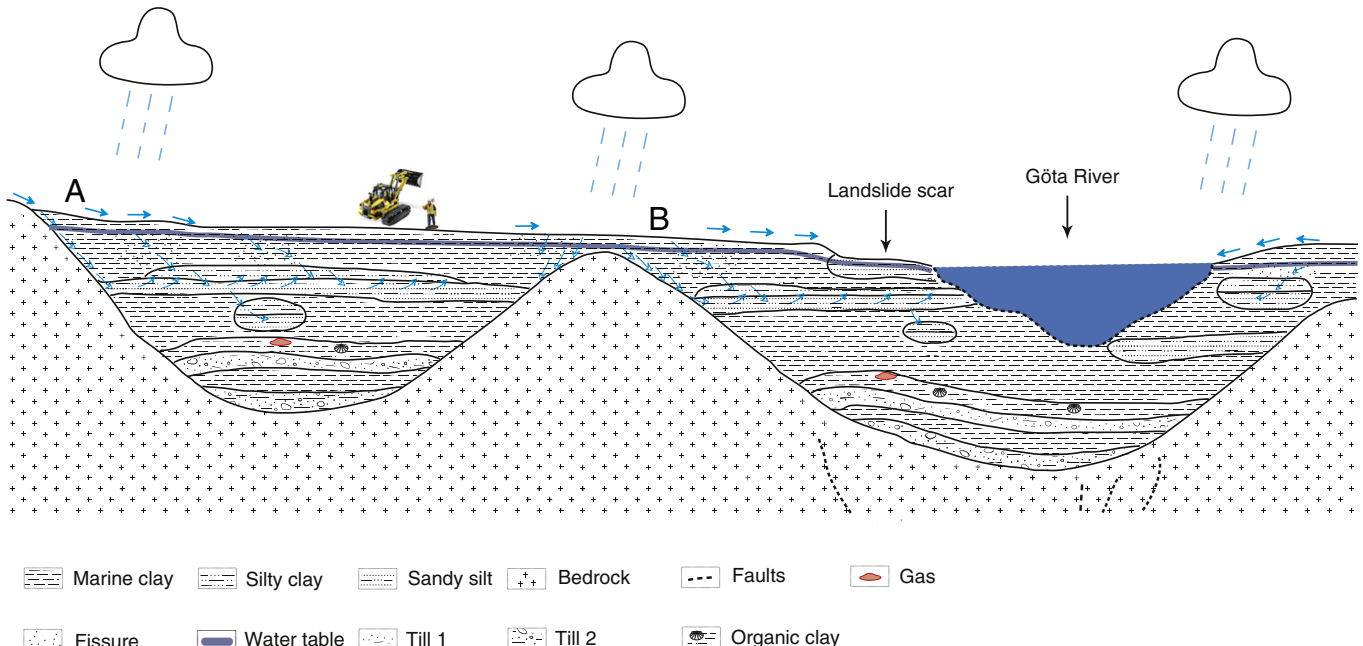


Fig. 13. Sketch showing possible role of the bedrock and coarse-grained materials in the formation of quick clays and their landslide triggering mechanism. Landslides in areas where the sediments are surrounded by the bowl-shaped bedrock (region A) would require removal of sediments or external sources like construction while in areas close to the river (region B) erosion in the river bank combined with increased or sudden change in the pore pressure in the coarse-grained materials would be enough to trigger quick-clay landslides. In either case, bedrock surface at highlands and on-lapping coarse-grained materials would facilitate the process and the formation of the quick clays.

accordance when compared to the existing cored and geotechnical boreholes, and reflection seismic data acquired in earlier studies. The data in particular enabled delineating the bedrock surface and its undulation, more importantly an interpretable large-scale coarse-grained layer (may also be patchy at some places) is overlapping the bedrock. Bedrock was found at about 150 m depth under the Göta River with much more overlapping sediments on the southern side of the river than the northern side.

While speculative, we conclude from the shape of the bedrock and the amount of sediments two different mechanisms for triggering quick-clay landslides at the site. In areas close to the river, erosion of the riverbank combined with increased pore pressure in the coarse-grained materials due to excess water and surface topography would likely be responsible for landslides. On the other hand, there is less chance of landslides in areas where the sediments are located in a bedrock depression, isolated from the river. In these areas human activity such as construction or settlement may destabilize the toe of the materials leading to a landslide. Future studies are required to validate these interpretations and to take advantages of joint inversion of both datasets for improved imaging and delineation of materials crucial for the formation of quick clays and the triggering of landslides.

Acknowledgments

This work is conducted within the frame of Trust 2.2 (Trust-GeoInfra: <http://www.trust-geoinfra.se/>) sponsored by Formas, SGU, BeFo, SBUF, Skanska, NGI and FQM. The Society of Exploration Geophysicists (SEG) through its Geoscientists Without Borders (GWB) program sponsored the 2011 geophysical studies for which we are grateful. We thank F. Zhang and A. Tryggvason for providing and helping with PS_tomo program, T. Kalscheuer and C. Shan for providing and helping with EMILIA program. S. Salas-Romero and S. Andersson contributed in the data acquisition and preparation of some of the data for which we are thankful. S. Wang thanks the China Scholarship Council (201306370039), Formas (25220121907), National Natural Science Foundation of China (D040901) and National High Technology Research and Development Program of China (2012AA09A20105) for supporting

his PhD study at Uppsala University. We thank A. Pfaffhuber and an anonymous reviewer for their critical and useful comments that improved an early version of this paper. We thank I. Snowball for kindly polishing our paper and providing very useful comments. We also thank the editor K. Wang for his helpful comments.

References

- AB Svensk Filmindustri, 1957. Veckorevy 1957-06-12, SVT. Available from: <http://www.filmarkivet.se/sv/Film/?movieid=336> (21 January 2016).
- Adamczyk, A., Malinowski, M., Malehmir, A., 2013. Application of first-arrival tomography to characterize a quick clay landslide site in Southwest Sweden. *Acta Geophys.* 61 (5), 1057–1073. <http://dx.doi.org/10.2478/s11600-013-0136-y>.
- Adamczyk, A., Malinowski, M., Malehmir, A., 2014. High-resolution near-surface velocity model building using full-waveform inversion—a case study from Southwest Sweden. *Geophys. J. Int.* 197, 1693–1704. <http://dx.doi.org/10.1093/gji/ggu070>.
- Andersson-Sköld, Y., Torrance, J.K., Lind, B., Ode'n, K., Stevens, R.L., Rankka, K., 2005a. Quick clay—a case study of chemical perspective in Southwest Sweden. *Eng. Geol.* 82, 107–118. <http://dx.doi.org/10.1016/j.enggeo.2005.09.014>.
- Andersson-Sköld, Y., Rankka, K., Lind, B., Ode'n, K., Torrance, J.K., Stevens, R.L., Dahlin, T., Leroux, V., 2005b. Quick clay—an investigation in Southwest Sweden. In: Senneiset, Flaate, Larsen (Eds.), *Landslides and Avalanches: ICFL 2005 Norway*. Taylor and Francis Group, London.
- Bastani, M., 2001. EnviroMT—A New Controlled Source/Radio Magnetotelluric System Ph.D. thesis Uppsala University, Uppsala.
- Bastani, M., Hübner, J., Kalscheuer, T., Pedersen, L.B., Godio, A., Bernard, J., 2012. 2D joint inversion of RMT and ERT data versus individual 3D inversion of full tensor RMT data: an example from Trecate site in Italy. *Geophysics* 77 (4), 233–243. <http://dx.doi.org/10.1190/GEO2011-0525.1>.
- Bastani, M., Persson, L., Mehta, S., Malehmir, A., 2015. Boat-towed radio-magnetotellurics—a new technique and case study from the city of Stockholm. *Geophysics* 80 (6), B193–B202. <http://dx.doi.org/10.1190/geo2014-0527.1>.
- Bazin, S., Pfaffhuber, A.A., 2013. Mapping of quick clay by electrical resistivity tomography under structural constraint. *J. Appl. Geophys.* 98, 280–287. <http://dx.doi.org/10.1016/j.jappgeo.2013.09.002>.
- Benz, H.M., Chouet, B.A., Dawson, P.B., Lahr, J.C., Page, R.A., Hole, J.A., 1996. Three dimensional P- and S-wave velocity structure of redoubt volcano, Alaska. *J. Geophys. Res.* 101, 8111–8128.
- Brand, E.W., Brenner, R.P., 1981. *Soft clay engineering* Ph.D. thesis Elsevier Scientific.
- Brodin, B., Malehmir, A., Juhlin, C., Dynesius, L., Bastani, M., Palm, H., 2015. Multicomponent broadband digital-based seismic landstreamer for near-surface applications. *J. Appl. Geophys.* 123, 227–241. <http://dx.doi.org/10.1016/j.jappgeo.2015.10.009>.
- Constable, S.C., Parker, R.L., Constable, C.G., 1987. Occam's inversion: a practical algorithm for generating smooth models from electromagnetic sounding data. *Geophysics* 52 (3), 289–300.

- Crozier, M.J., 2010. Landslide geomorphology: an argument for recognition, with examples from New Zealand. *Geomorphology* 120, 3–15. <http://dx.doi.org/10.1016/j.geomorph.2009.09.010>.
- Dahlin, T., Löfroth, H., Schälin, D., Seur, P., 2013. Mapping of quick clay using geoelectrical imaging and CPTU-resistivity. *Near Surf. Geophys.* 11, 659–670. <http://dx.doi.org/10.3997/1873-0604.2013044>.
- Donohue, S., Long, M., O'Connor, P., Eide-Helle, T., Pfaffhuber, A.A., Rømoen, M., 2012. Multi-method mapping of quick-clay. *Near Surf. Geophys.* 10 (3), 207–219. <http://dx.doi.org/10.3997/1873-0604.2012003>.
- Geertsema, M., Torrance, J.K., 2005. Quick clay from the Mink Creek landslide near Terrace, British Columbia: geotechnical properties, mineralogy, and geochemistry. *Can. Geotech. J.* 42, 907–918. <http://dx.doi.org/10.1139/T05-028>.
- Gregersen, O., 1981. *The quick landslide in Rissa, Norway. The sliding process and discussion of failure modes*. Norw. Geotech. Inst. 135, 1–6 (Oslo).
- Gregersen, O., Løken, T., 1979. *The quick-clay slide at Baestad, Norway*, 1974. Eng. Geol. 14, 183–196.
- Helle, T.E., Nordal, S., Aagaard, P., Lied, O.K., 2015. Long-term effect of potassium chloride treatment on improving the soil behaviour of highly sensitive clay—Ulvensplitten, Norway. *Can. Geotech. J.* 52, 1–13. <http://dx.doi.org/10.1139/cgj-2015-0077>.
- Hibert, C., Grandjean, G., Bitri, A., Travelletti, J., Malet, J.P., 2012. Characterizing landslides through geophysical data fusion: example of the La Valette landslide (France). *Eng. Geol.* 128, 23–29. <http://dx.doi.org/10.1016/j.enggeo.2011.05.001>.
- Highland, L.M., Bobrowsky, P., 2008. *The Landslide Handbook – a Guide to Understanding Landslides*. U.S. Geological Survey, Reston, Virginia.
- Hole, J.A., Zelt, B.C., 1995. 3-D finite-difference reflection traveltimes. *Geophys. J. Int.* 121, 427–434. <http://dx.doi.org/10.1111/j.1365-246X.1995.tb05723.x>.
- Kalscheuer, T., Pedersen, L.B., Siripunvaraporn, W., 2008. Radiomagnetotelluric two-dimensional forward and inverse modelling accounting for displacement currents. *Geophys. J. Int.* 175 (2), 486–514.
- Kalscheuer, T., Bastani, M., Donohue, S., Persson, L., Pfaffhuber, A.A., Reiser, F., Ren, Z., 2013. Delineation of a quick clay zone at Smorgrav, Norway, with electromagnetic methods under geotechnical constraints. *J. Appl. Geophys.* 92, 121–136. <http://dx.doi.org/10.1111/j.1365-246X.2008.03902.x>.
- Krawczyk, C.M., Polom, U., Malehmir, A., Bastani, M., 2013. Quick-clay landslides in Sweden—insights from shear-wave reflection seismics and geotechnical integration. *Near Surface Geoscience*, 19th EAGE European Meeting of Environmental and Engineering Geophysics, Bochum <http://dx.doi.org/10.3997/2214-4609.20131348>.
- Löfroth, H., Suer, P., Dahlin, T., Leroux, V., Schälin, D., 2011. Quick-clay mapping by resistivity-surface resistivity, CPTU-R and chemistry to complement other geotechnical sounding and sampling. Swedish Geotechnical Institute, report GÅU 30, Linköping.
- Long, M., Donohue, S., L'Heureux, J.-S., Solberg, I.-L., Ronning, J.S., Limacher, R., O'Connor, P., Sauvin, G., Rømoen, M., Lecomte, I., 2012. Relationship between electrical resistivity and basic geotechnical parameters for marine clays. *Can. Geotech. J.* 49, 1158–1168. <http://dx.doi.org/10.1139/T2012-080>.
- Lundberg, E., Malehmir, A., Juhlén, C., Bastani, M., Andersson, M., 2014. High-resolution 3D reflection seismic investigation over a quick-clay landslide scar in Southwest Sweden. *Geophysics* 79 (2), B97–B107. <http://dx.doi.org/10.1190/GEO2013-0225.1>.
- Lundström, K., Larsson, R., Dahlin, T., 2009. Mapping of quick clay formations using geotechnical and geophysical methods. *Landslides* 6, 1–15. <http://dx.doi.org/10.1007/s10346-009-0144-9>.
- Malehmir, A., Bastani, M., Krawczyk, C., Gurk, M., Ismail, N., Polom, U., Persson, L., 2013a. Geophysical assessment and geotechnical investigation of quick-clay landslides—a Swedish case study. *Near Surf. Geophys.* 11, 341–350. <http://dx.doi.org/10.3997/1873-0604.2013010>.
- Malehmir, A., Saleem, M.U., Bastani, M., 2013b. High-resolution reflection seismic investigations of quick-clay and associated formations at a landslide scar in Southwest Sweden. *J. Appl. Geophys.* 92, 84–102. <http://dx.doi.org/10.1016/j.jappgeo.2013.02.013>.
- Malehmir, A., Andersson, M., Mehta, S., Brodic, B., Munier, R., Place, J., Maries, G., Smith, C., Kamm, J., Bastani, M., Mikko, H., Lund, B., 2016. Post-glacial reactivation of the Bollnäs fault, Central Sweden. *Solid Earth* 7, 509–527. <http://dx.doi.org/10.5194/se-7-509-2016>.
- Malehmir, A., Zhang, F., Dehgahnnejad, M., Lundberg, E., Döse, C., Friberg, O., Brodic, B., Place, J., Svensson, M., Möller, H., 2015. Planning of urban underground infrastructure using a broadband seismic landstreamer—tomography results and uncertainty quantifications from a case study in southwest of Sweden. *Geophysics* 80, B177–B192. <http://dx.doi.org/10.1190/GEO2015-0052.1>.
- Moorkamp, M., Heincke, B., Jegen, M., Roberts, A.W., Hobbs, R.W., 2013. A framework for 3-D joint inversion of MT, gravity and seismic refraction data. *Geophys. J. Int.* 184, 477–493. <http://dx.doi.org/10.1111/j.1365-246X.2010.04856.x>.
- Nabighian, M.N., 1987. *Electromagnetic Methods in Applied Geophysics—Theory* vol. 1. United States of America.
- Nadim, F., Pedersen, S.A.S., Schmidt-Thomé, P., Sigmundsson, F., Engdahl, M., 2008. *Natural hazards in Nordic countries*. Episodes 31, 176–184.
- Paige, C.C., Saunders, M.A., 1982. LSQR: an algorithm for sparse linear equations and sparse least squares. *ACM Trans. Math. Softw.* 8 (1), 43–71.
- Pedersen, L.B., Engels, M., 2005. Routine 2D inversion of magnetotelluric data using the determinant of the impedance tensor. *Geophysics* 70 (2), G33–G41. <http://dx.doi.org/10.1190/1.1897032>.
- Pedersen, L.B., Bastani, M., Dynesius, L., 2006. Some characteristics of the electromagnetic field from radiotransmitters in Europe. *Geophysics* 71, 279–284. <http://dx.doi.org/10.1190/1.2349222>.
- Persson, M.A., Stevens, R.L., Lemoine, Å., 2014. Spatial quick-clay predictions using multi-criteria evaluation in SW Sweden. *Landslides* 11, 263–279. <http://dx.doi.org/10.1007/s10346-013-0385-5>.
- Pfaffhuber, A.A., Bastani, M., Cornée, S., Rømoen, M., Donohue, S., Helle, T.E., Long, M., O'Connor, P., Persson, L., 2010. Multi-method high resolution geophysical & geotechnical quick clay mapping. Near Surface 2010—16th European Meeting of Environmental and Engineering Geophysics Zurich, Switzerland.
- Pfaffhuber, A.A., Bazin, S., Helle, T.E., 2014. An integrated approach to quick-clay mapping based on resistivity measurements and geotechnical investigations. *Advan. Nat. Technol. Haz. Res.* 36, 193–204. http://dx.doi.org/10.1007/978-94-007-7079-9_15.
- Podvin, P., Lecomte, I., 1991. Finite difference computation of traveltimes in very contrasted velocity models: a massively parallel approach and its associated tools. *Geophys. J. Int.* 105 (1), 271–284. <http://dx.doi.org/10.1111/j.1365-246X.1991.tb03461.x>.
- Rankka, K., Andersson-Sköld, Y., Hultén, C., Larsson, R., Leroux, V., Dahlin, T., 2004. Quick-clay in Sweden. Swedish Geotechnical Institute, technical report number 65, p. 137 (Linköping).
- Rømoen, M., Pfaffhuber, A.A., Karlrud, K., Helle, T.E., 2010. Resistivity on marine sediments retrieved from RCPTU-sounding: a Norwegian case study. 2nd International Symposium on Cone Penetration Testing, CPT'10, Huntington Beach, CA. Proceeding 2, pp. 289–296.
- Rudberg, S., 1997. Sweden. In: Embleton, C.C. (Ed.), *Geomorphological Hazards of Europe*. Elsevier Press, Amsterdam.
- Salas-Romero, S., Malehmir, A., Snowball, I., Lougheed, B.C., Hellqvist, M., 2015. Identifying landslide preconditions in Swedish quick clays—insights from integration of surface geophysical, core sample and downhole property measurement. *Landslide* <http://dx.doi.org/10.1007/s10346-015-0633-y>.
- Sauvin, G., Lecomte, I., Bazin, S., Hansen, L., Vanneste, M., L'Heureux, J., 2014. On the integrated use of geophysics for quick-clay mapping: the Hvittingfoss case study, Norway. *J. Appl. Geophys.* 106, 1–13. <http://dx.doi.org/10.1016/j.jappgeo.2014.04.001>.
- Shan, C., Bastani, M., Malehmir, A., Persson, L., Engdahl, M., 2014. Integrated 2D modeling and interpretation of geophysical and geotechnical data to image quick-clays at a landslide site in Southwest Sweden. *Geophysics* 79 (4), EN61–EN75. <http://dx.doi.org/10.1190/GEO2013-0201.1>.
- Shan, C., Bastani, M., Malehmir, A., Persson, L., Lundberg, E., 2016. Integration of controlled-source and radio magnetotellurics, electric resistivity tomography, and reflection seismics to delineate 3D structures of a quick-clay landslide site in southwest of Sweden. *Geophysics* 81 (1), B13–B29. <http://dx.doi.org/10.1190/GEO2014-0386.1>.
- Siripunvaraporn, W., Egbert, G., 2000. An efficient data-subspace inversion method for 2D magnetotelluric data. *Geophysics* 65 (3), 791–803.
- Solberg, I., 2007. *Geological, geomorphological and geophysical investigations of areas prone to clay slides: examples from Buvika, Mid Norway*. Ph.D. thesis Norwegian University of Science and Technology, Trondheim.
- Solberg, I., Hansen, L., Ronning, J.S., Haugen, E.D., Dalsegg, E., Tønnesen, J.F., 2012. Combined geophysical and geotechnical approach to ground investigations and hazard zonation of a quick-clay area, mid Norway. *Bull. Eng. Environ.* 71, 119–133. <http://dx.doi.org/10.1007/s10064-011-0363-x>.
- Spies, B.R., 1989. Depth of investigation in electromagnetic sounding methods. *Geophysics* 54 (7), 872–888.
- Tezkan, B., Goldman, M., Greinwald, S., Hördt, A., Neubauer, F.M., Zacher, G., 1996. A joint application of radiomagnetotellurics and transient electromagnetics to investigation of a waste deposit in Cologne (Germany). *J. Appl. Geophys.* 34, 199–212.
- Torrance, J.K., 2012. *Landslides in quick clay*. In: Clague, J.J., Stead, D. (Eds.), *Landslides: Types, Mechanisms and Modelling*. Cambridge University Press, Cambridge.
- Torrance, J.K., 2014. Chemistry, sensitivity and quick-clay landslide amelioration. In: L'Heureux, J.-S., Locat, A., Leroueil, S., Demers, D., Locat, J. (Eds.), *Landslides in Sensitive Clays*. Springer Press, New York London.
- Tryggvason, A., Rögnvaldsson, S.Th., Flóvenz, Ó.G., 2002. Three-dimensional imaging of the P- and S-wave velocity structure and earthquake locations beneath Southwest Iceland. *Geophys. J. Int.* 151 (3), 848–866.